Exploring the Macroevolutionary Signature of Asymmetric Inheritance at Speciation

Théo Gaboriau[1,*], Joseph A. Tobias[2] Daniele Silvestro[3,4,5,6] and Nicolas Salamin[1]

[1] *Department of Computational Biology, University of Lausanne, Lausanne, Switzerland*
[2] *Department of Life Sciences, Imperial College London, Silwood Park, Ascot, UK*
[3] *Gothenburg Global Biodiversity Centre, Gothenburg, Sweden*
[4] *Department of Biological and Environmental Sciences, University of Gothenburg, Gothenburg, Sweden*
[5] *Department of Biology, University of Fribourg, Fribourg, Switzerland*
[6] *Swiss Institute of Bioinformatics, Fribourg, Switzerland*

**theo.gaboriau@unil.ch*

Abstract

Popular comparative phylogenetic models such as Brownian Motion, Ornstein-Ulhenbeck, and their extensions, assume that, at speciation, a trait value is inherited identically by two descendant species. This assumption contrasts with models of speciation at a micro-evolutionary scale where descendants' phenotypic distributions are sub-samples of the ancestral distribution. Different speciation mechanisms can lead to a displacement of the ancestral phenotypic mean among descendants and an asymmetric inheritance of the ancestral phenotypic variance. In contrast, even macro-evolutionary models that account for intraspecific variance assume symmetrically conserved inheritance of ancestral phenotypic distribution at speciation. Here we develop an Asymmetric Brownian Motion model (ABM) that relaxes the assumption of symmetric and conserved inheritance of the ancestral distribution at the time of speciation. The ABM jointly models the evolution of both intra- and inter-specific phenotypic variation. It also infers the mode of phenotypic inheritance at speciation, which can range from a symmetric and conserved inheritance, where descendants inherit the ancestral distribution, to an asymmetric and displaced inheritance, where descendants inherit divergent phenotypic means and variances. To demonstrate this model, we analyze the evolution of beak morphology in Darwin finches, finding evidence of displacement at speciation. The ABM model helps to bridge micro- and macro-evolutionary models of trait evolution by providing a more robust framework for testing the effects of ecological speciation, character displacement, and niche partitioning on trait evolution at the macro-evolutionary scale.

Key words: Character displacement, Phenotypic evolution, Phylogenetic comparative methods, Speciation

Introduction

Models describing the evolution of phenotypic traits on phylogenetic trees are core elements of Phylogenetic Comparative Methods (PCM) and crucial tools for understanding processes shaping biodiversity. Most of these models can be described as multivariate stochastic processes using the underlying phylogenetic tree to describe covariance between species (Lande, 1980b; Felsenstein, 1985). The plethora of new PCM developed in recent years illustrates the importance of these methods in modern macroevolutionary research and allows modelling trait evolution as neutral (Brownian motion, Felsenstein (1973)), attracted towards one or multiple optima (Ornstein-Ulhenbeck, Hansen (1997); Khabbazian et al. (2016)), drifting with a trend (Silvestro et al., 2019) or diverging away from interacting clades (Drury et al., 2016). Models are also able to incorporate evolutionary rates variation through time (Harmon et al., 2010a), among clades (Beaulieu et al., 2012; Castiglione et al., 2018), or with respect to environmental changes (Clavel and Morlon, 2017), other traits (Hansen et al., 2021), or substitution rates (Lartillot and Poujol, 2011).

One underlying and often neglected assumption of these models is the symmetric and complete inheritance of the ancestors' phenotype by its descendants at a branching event. This assumption is rooted in two characteristics of the PCM. First, phylogenetic trees represent speciation as an instantaneous event in time (Mendes et al., 2018). Second, PCM generally models the evolution of mean phenotypes, ignoring the intraspecific variation. Models incorporating intraspecific trait variance either treat it as a measurement error (Harmon and Losos, 2005) or model its evolution independently of the trait mean (Kostikova et al., 2016; Gaboriau et al., 2020).

Given these structural constraints, it is challenging to consider within the current PCM the progressive nature of the speciation process and its effect on the trait distribution of the descendants. This assumption contrasts with the classic description of speciation at the micro-evolutionary scale (Simpson, 1953; Mayr, 1963; Lande, 1980a; Gavrilets, 2014),

in which accelerated trait divergence is often associated with speciation (cladogenetic change). In the context of neutral divergence, descendant species are sub-samples of the parent species population. Differences between incipient species phenotypic distributions are therefore expected by chance (Duchen et al., 2021), especially in the case of peripatric and parapatric speciation where one of the incipient species originates as a small non-random subset of the parent population size with therefore more chances to diverge from the ancestral trait distribution (Schwämmle et al., 2006; Kopp, 2010). Alternatively, the speciation process can directly be associated with trait divergence. For instance, dispersing to a new region or environment can increase the probability of speciation because of reduced gene flow, trait divergence by local adaptation, and/or ecological opportunity (Simpson, 1953; Mayr, 1963; Eastman et al., 2013). Island radiations provide striking empirical evidence of this scenario (Losos et al., 2003; Grant and Grant, 2008) with accelerated phenotypic divergence at the time of speciation (Eastman et al., 2013). Other ecological opportunities, such as the extinction of potential competitors or the emergence of a key innovation, are also hypothesized to cause rapid divergence by disruptive selection, leading to sympatric speciation (Gavrilets, 2003; Ackermann and Doebeli, 2004). Given this range of speciation scenarios (Fig. 1), the assumption of equal inheritance of a trait at speciation is likely to be violated, and simulations show this can lead to biased macroevolutionary estimates (Duchen et al., 2021).

Fig. 1. Different scenarios of ancestral distribution's inheritance are expected depending on the processes that caused segregation. Each line represents a different speciation scenario from the same ancestral population (top left) with intraspecific variation. The measured phenotype is body-size as represented by different sizes of bird images. The central column represents simulations of how ancestral and descendant species distributions change through time. Lines represent the evolution of the mean, and shaded polygons represent the 95% interval of each species distribution. T_s is the time of speciation represented as a branching event in a phylogeny. The ancestral distribution is represented in black and the descendants in orange and blue. The right column represents the expected distributions of descendants' phenotypes at the time of speciation T_s according to the ABM model. The parameters ν (asymmetry) and ω (displacement) control the repartition of the ancestral distribution (in black) into two descending distributions in blue and orange.

Several models can test for bursts in evolutionary rates at the macroevolutionary scale by modeling anagenetic rates variation (Blomberg et al., 2003; Harmon et al., 2010b)

or evolutionary jumps (Landis et al., 2013; Eastman et al., 2013; Duchen et al., 2017). Although they can detect changing rates of phenotypic evolution or phenotypic jumps, those models do not consider cladogenetic changes and might fail to capture its signal. Other methods attempt to decouple anagenetic change from cladogenetic change. The κ statistic tests the relationship between branch lengths and evolutionary rates, with $\kappa < 1$ indicating a faster phenotypic change at speciation than near the tips (Pagel, 1999). Another method proposed to independently model anagenetic and cladogenetic evolutionary rates while incorporating the probability of speciation events masked by extinction, (Bokma, 2008). Whether these methods identify the signal of cladogenetic changes or capture periods of accelerated anagenetic evolution remains unclear.

An alternative approach to modeling trait evolution uses measurements across multiple individuals per species as input data to jointly infer phenotypic mean evolution across species and evolution of its intraspecific variance (Kostikova et al., 2016; Gaboriau et al., 2020). While this approach unlocks the possibility to model explicitly how the ancestral trait distribution is inherited by descendent lineages, its current implementation makes the simplifying assumptions that 1) trait means and variance evolve independently and 2) they are identically inherited at speciation.

Here, we posit that cladogenetic changes due to asymmetric inheritance at speciation leave a signature in present species trait distribution. Thus, a joint analysis of the evolution of trait mean and variance can reveal the mode of cladogenetic trait inheritance (Fig. 1). We develop a new method to model both cladogenetic and anagenetic changes of phenotypic distribution and test it on simulated and empirical data.

Materials and Methods

An Asymmetric Brownian motion model

We developed a new model of trait evolution that accounts for the non-independent

change over time of its mean value and intraspecific variance while introducing a gradient of inheritance scenarios that can occur at speciation event and that will affect the way the ancestral trait is passed onto two descendants (Fig. 1). We model the evolution of both trait variances and trait means along the branches of a tree based on two independent Brownian processes. We assume that the speciation process, represented by a dichotomous branching in the phylogenetic tree, can split the ancestral distribution into two distinct distributions in the descendants. This process is modulated by two parameters: ν controls the asymmetry between trait variances inherited by the two descendants and ω controls the displacement between the descendants trait means. A $\nu > 0$ indicates that one descendant inherits a smaller part of the ancestral variance than the other (Fig. 1.b,d). A $\nu = 0$ indicates that both descendants inherit the same amount of ancestral variance (Fig. 1.a,c). An $\omega > 0$ indicates that the descendants inherit different parts of the ancestral distribution (Fig. 1.c,d), leading to a cladogenetic change in phenotypic means and variances. An $\omega = 0$ corresponds to an evolutionary scenario where identical phenotypic means are inherited at speciation (Fig. 1.a,b). The cladogenetic changes implemented in this model are described as functions of the ancestral distribution at the time of speciation and conserve features of the ancestral distribution (i.e. 5% and 95% quantiles, variance) in the union of the two inherited distributions. Therefore, scenarios implying a partial loss of the ancestral distribution during the speciation process are not covered by our model. The current implementation of the model also assumes that ν and ω are constant among nodes. We assess the consequences of these assumptions later in the manuscript and discuss their implications.

Asymmetry and/or displacement at the time of speciation create a disjunction between descendants' distribution that is controlled by "switch" parameters at each node of the phylogenetic tree. Independent switch parameters are assigned to each node in the tree and can take the value of 1 or -1, determining which descendant inherits the smaller

part of the ancestral variance (S_ν) if $\nu > 0$ and which descendant inherits the lower ancestral quantiles and therefore lower mean (S_ω) if $\omega > 0$. The ancestral distribution at nodes and switch parameters are estimated using data augmentation conditional on present species distributions, phylogenetic tree and other parameters. In the sections below we provide a more detailed description of the ABM model and its implementation.

Model definition

We assume that the trait intraspecific distribution is normally distributed. Along branches, we independently model the evolution of the intraspecific phenotypic means and log variances based on Brownian processes following standard phylogenetic comparative approaches. At the time of a speciation event (T_s), represented as a dichotomy in a phylogenetic tree, we first assume that the ancestral distribution (X_a) shares its 5^{th} and 95^{th} percentiles respectively with at least one of the descendants' distributions (X_{1_s}, X_{2_s}, Fig. 1).

$$\begin{cases} Q_{0.05}(X_a) = \min(Q_{0.05}(X_{1_s}), Q_{0.05}(X_{2_s})) \\ Q_{0.95}(X_a) = \max(Q_{0.95}(X_{1_s}), Q_{0.95}(X_{2_s})) \end{cases}$$

We calculate the 5^{th} and 95^{th} quantiles of a normal distribution ($X \sim \mathcal{N}(\mu, \sigma)$) using the inverse error function ($\text{erf}^{-1}(\cdot)$) :

$$\begin{cases} Q_{0.05}(X) = \mu - \Phi^{-1}\sigma \\ Q_{0.95}(X) = \mu + \Phi^{-1}\sigma \end{cases}$$

with $\Phi^{-1} = \sqrt{2}\text{erf}^{-1}(0.9)$

We can define the quantiles of an ancestral species distribution as a function of the two descendant species variances:

$$\begin{cases} \mu_a - \Phi^{-1}\sigma_a &= \min(\mu_{1_s} - \Phi^{-1}\sigma_{1_s}, \mu_{2_s} - \Phi^{-1}\sigma_{2_s}) \\ \mu_a + \Phi^{-1}\sigma_a &= \max(\mu_{1_s} + \Phi^{-1}\sigma_{1_s}, \mu_{2_s} + \Phi^{-1}\sigma_{2_s}) \end{cases} \tag{0.1}$$

where μ_a is the mean of the ancestral distribution at the time of speciation, σ_a is the standard deviation of the ancestral distribution at the time of speciation, and (μ_{1_s}, μ_{2_s}) and $(\sigma_{1_s}, \sigma_{2_s})$ are the means and standard deviations of the descendants distributions at the time of speciation. This equation ensures that at least one of the descendants distributions respectively shares the 5^{th} and 95^{th} quantiles of the ancestral distribution.

Second, we postulate that the descendants distributions might inherit the ancestral variance asymmetrically. Asymmetry between trait variances of the two descendants is denoted by $\nu \in [0, 1)$ as follows:

$$\nu = \frac{S_{\nu_1}\sigma_{1_s} + S_{\nu_2}\sigma_{2_s}}{\sigma_a} \tag{0.2}$$

where the switch parameters $S_{\nu_1} \in \{-1, 1\}$ and $S_{\nu_2} = -S_{\nu_1}$ are indicators to specify which descendant inherits the larger part of the ancestral variance. Lineages associated with a $S_\nu = -1$ lost a part of the ancestral variance during speciation if $\nu > 0$. The sister lineage thus gets a value of $S_\nu = 1$ and inherits a larger part of the ancestral variance. Under this definition, a value of $\nu = 0$ indicates a symmetric inheritance of the ancestral variance, while asymmetry grows when ν becomes closer to 1. This equation further constrains the difference between the descendants variances to be lower than the ancestral variance. This constraint ensures that each descendant variance is lower or equal to the ancestral variance. However, ν cannot be 1 as it would mean that one of the descendants has a null variance.

Third, trait segregation might occur at speciation. Under this process, descendants inherit different parts of the ancestral distribution. We measure this process by introducing a parameter $\omega \in [0, 1]$, which represents the displacement between descendants' mean trait values such that:

$$\omega = \frac{S_{\omega_1}\mu_{1_s} + S_{\omega_2}\mu_{2_s}}{\Phi^{-1}(2 - \nu)\sigma_a} \tag{0.3}$$

The switch parameters $S_{\omega_1} \in \{-1, 1\}$ and $S_{\omega_2} = -S_{\omega_1}$ indicate, again, which of the two descendants inherits the highest mean value. Under this definition, $\omega = 0$ indicates no

displacement between descendants, while $\omega = 1$ represents the maximum possible displacement, given Eq. 0.1. Lineages associated with a $S_\omega = -1$ experienced a cladogenetic decrease of their phenotype if $\omega > 0$. The sister lineage thus gets a value of $S_\omega = 1$ and experiences a cladogenetic increase of their phenotype. The term $\Phi^{-1}(2-\nu)\sigma_a$ ensures that the expression of ω is compatible with our first hypothesis. If there is asymmetry ($\nu > 0$), displacement has to be lower than the ancestral distribution's 95^{th} interval for the descendants' distributions 5^{th} and 95^{th} quantiles to remain in that interval. This way, descendants' means are constrained by the ancestral variance and cannot lie outside the ancestral distribution. These equations (Eqs 0.1, 0.2, 0.3) cover a continuum between alternative inheritance scenarios of the ancestral distribution at speciation (Fig. 1,A2).

Likelihood of the interspecific distribution

We derive the likelihood of phenotypic means and variances across species given a phylogenetic tree and one or more trait observations per species. We start by showing the calculations on a simple tree with two species sharing a common ancestor. Using Eqn. 0.2 and 0.3, we can express the descendants' mean and variance as a function of ancestral values, ν, and ω (see the complete derivation in supplementary methods):

$$\begin{cases} \sigma_{i_s} = & \sigma_a \times \mathcal{S}(S_{\nu_i}) \\ \mu_{i_s} = & \mu_a + \sigma_a \times \mathcal{M}(S_{\nu_i}, S_{\omega_i}) \end{cases} \tag{0.4}$$

where

$$\begin{cases} \mathcal{S}(S_{\nu_i}) & = \frac{1}{2} \times (2 + \min(0, S_{\nu_i}\nu + \omega(2-\nu)) + \min(0, S_{\nu_i}\nu - \omega(2-\nu))) \\ \mathcal{M}(S_{\nu_i}, S_{\omega_i}) & = \frac{1}{2}\Phi^{-1} \times (\min(0, S_{\nu_i}\nu + S_{\omega_i}\omega(2-\nu)) - \min(0, S_{\nu_i}\nu - S_{\omega_i}\omega(2-\nu))) \end{cases} \tag{0.5}$$

$\mathcal{S}(S_{\nu_i}) \in (0, 1]$ determines the proportion of ancestral variance inherited by descendant i. In the case of asymmetry, S_{ν_i} controls whether species i inherits the smaller ($S_{\nu_i} = -1$) or bigger ($S_{\nu_i} = 1$) proportion of ancestral variance. Its sister clade will inherit a proportion of ancestral variance equal to $\mathcal{S}(-S_{\nu_i})$. Similarly, $\mathcal{M}(S_{\nu_i}, S_{\omega_i}) \in [-1.96, 1.96]$ determines

the distance between the ancestral mean and descendant i mean in terms of ancestral standard deviation units. If $S_{\omega_i} = -1$, μ_i is smaller or equal to the ancestral mean, if $S_{\omega_i} = 1$, μ_i is bigger or equal to the ancestral mean. We consider that means and variances of each species evolve independently along the branches of the phylogenetic tree following a Brownian process (Felsenstein, 1985). We model the evolution of the logarithm of the standard deviation ($\log(\sigma)$, hereafter noted ζ) as implemented in the JIVE model (Kostikova et al., 2016; Gaboriau et al., 2020). At a speciation event, represented by a node in the phylogenetic tree, we infer descendants' distributions and obtain expectations of ζ_1, ζ_2, μ_1 and μ_2 for extant species under our model using Eqn. 0.4:

$$\begin{cases} E[\zeta_i] = & \zeta_a + \log \mathcal{S}(S_{\nu_i}) \\ E[\mu_i] = & \mu_a + \sigma_a \times \mathcal{M}(S_{\nu_i}, S_{\omega_i}) \end{cases}$$

Even though asymmetry and displacement modify expectations for our variables, their variances are not affected by the deterministic process. Thus, we can derive variances from the standard Brownian process:

$$\begin{cases} V[\zeta_i] = & \gamma_i \sigma_\zeta^2 \\ V[\mu_i] = & \gamma_i \sigma_\mu^2 \end{cases}$$

where γ_i is the branch length leading to species i, and σ_ζ^2 and σ_μ^2 are evolutionary rates of ζ and μ, respectively. These terms allow us to calculate the probability of $\sigma_1, \sigma_2, \mu_1$ and μ_2 given $\omega, \nu, \sigma_{a_s}, \mu_{a_s}, \sigma_\mu^2$ and σ_ζ^2 along a phylogenetic tree (Hansen, 1997). For a binary phylogenetic tree with n extant species and $n-1$ ancestral nodes all characterized by their trait distribution $X_i \sim \mathcal{N}(\mu_i, \sigma_i)$, we make the simplifying assumption that ν and ω are constant across every node with a different value for S_{ν_i} and S_{ω_i}. By applying (0.4) to each node and a BM process to each branch, we obtain (see the proof in supplementary methods):

$$E[\zeta_i] = \zeta_{\text{root}} + \sum_{j=1}^{J} \log \mathcal{S}(S_{\nu_j}) \tag{0.6}$$

$$E[\mu_i] = \mu_{\text{root}} + \sum_{j=1}^{J} \sigma_{a_j} \mathcal{M}(S_{\nu_j}, S_{\omega_j}) \tag{0.7}$$

with J being the number of branches between the root and species i and σ_{a_j} being the standard deviation of j's direct ancestor at speciation. We note that, with fixed σ_i, S_{ν_i} and S_{ω_i}, the variances of $\boldsymbol{\mu}$ and $\boldsymbol{\zeta}$ are not affected by the cladogenetic process, allowing us to use the standard phylogenetic variance-covariance matrix in our calculations. Using $E[\mu_i], E[\zeta_i], V[\mu_i]$ and $V[\zeta_i]$ we can calculate the likelihood functions of $\boldsymbol{\mu}$ and $\boldsymbol{\zeta}$ as multivariate normal distributions (Hansen, 1997).

$$\begin{aligned}\mathcal{L}(\theta|\nu, \omega, \sigma_\mu^2, \sigma_\zeta^2, \mu_{\text{root}}, \boldsymbol{\zeta'}, \boldsymbol{S_\nu}, \boldsymbol{S_\omega}, \boldsymbol{\gamma}) \\ \propto P(\boldsymbol{\zeta}|\nu, \omega, \sigma_\mu^2, \sigma_\zeta^2, \boldsymbol{\zeta'}, \boldsymbol{S_\nu}, \boldsymbol{S_\omega}, \boldsymbol{\gamma}) \\ \times P(\boldsymbol{\mu}|\nu, \omega, \sigma_\mu^2, \sigma_\zeta^2, \mu_{\text{root}}, \boldsymbol{\zeta'}, \boldsymbol{S_\nu}, \boldsymbol{S_\omega}, \boldsymbol{\gamma})\end{aligned}$$

where $\boldsymbol{\mu}$ and $\boldsymbol{\zeta}$ are observed means and log standard deviations. $\boldsymbol{\zeta'}$ and $\boldsymbol{\gamma}$ indicate the vector of all ancestral log standard deviations and branch lengths, respectively.

Parameter estimation

The Bayesian estimation of asymmetry (ν), displacement (ω) and evolutionary rates ($\sigma_\mu^2, \sigma_\zeta^2$) depend on the approximation of ancestral states ($\boldsymbol{\zeta'}, \mu_{\text{root}}$) and switch parameters ($\boldsymbol{S_\nu}, \boldsymbol{S_\omega}$). These parameters can be estimated using Gibbs sampling by calculating their conditional distributions on ν, ω, σ_μ^2 and σ_ζ^2. Specifically, we can show that, for any node k, the ancestral intraspecific log standard deviation ζ_k is a linear function of its descendants ζ (see supplementary methods for the proof). Therefore, for every node k with I_k extant descendants and J_k descending edges, we have:

$$\begin{aligned}&\zeta_k \sim \mathcal{N}(E[\zeta_k], V[\zeta_k]), \text{ with} \\ &E[\zeta_k] = \sum_{i=1}^{I_k} \frac{1}{2^{n_i}} (E[\zeta_i] + \frac{1}{2} C) \text{ and} \\ &V[\zeta_k] = \sum_{j=1}^{J_k} \frac{1}{4^{n_j}} \gamma_j \sigma_\zeta^2\end{aligned} \tag{0.8}$$

Where n_i and n_j are, respectively, the number of nodes between node k and i, j, and C is a constant for fixed ω and ν. For every node with direct descendants a and b we can also write:

$$\begin{aligned} P(S_{\nu_a} = 1) &\propto P(\zeta_a - \zeta_b > 0) \\ X_i &\sim \mathcal{N}(E[\zeta_a] - E[\zeta_b], V[\zeta_a] + V[\zeta_b]) \end{aligned} \tag{0.9}$$

The variable X_i can be used to calculate the conditional probability of $S_{\nu_i} = 1$.

After the sampling of $\boldsymbol{\zeta'}$ and $\boldsymbol{S_\nu}$ from their respective conditional distributions, we can calculate the conditional distribution of $\boldsymbol{\mu'}$ and $\boldsymbol{S_\omega}$. Similarly, for mean values, we can show that for any node k, μ_k is a linear combination of its descendants μ (see supplementary methods for the proof). Therefore, for any node k with I_k descendants and J_k descending branches, we have:

$$\begin{aligned} \mu_k &\sim \mathcal{N}(E[\mu_k], V[\mu_k]) \\ E[\mu_k] &= \sum_{i=1}^{I_k} (E[\mu_i] \prod_{j}^{J_k} w_j) \\ V[\mu_k] &= \sum_{j=1}^{J_k} w_j^2 \gamma_j \sigma_\mu^2 \end{aligned} \tag{0.10}$$

where w_j is a constant for fixed ω, ν and s_{ν_j} (see proof in supplementary methods). For every node with direct descendants a and b, we can also write:

$$\begin{aligned} P(S_{\omega_a} = 1) &\propto P(\mu_a - \mu_b > 0) \\ Y_a &\sim \mathcal{N}(E[\mu_b] - E[\mu_b], V[\mu_a] + V[\mu_b]) \end{aligned} \tag{0.11}$$

The variable Y_i can be used to calculate the conditional probability of $S_{\omega_i} = 1$. These expressions of conditional distribution for ancestral means, variances, and switch parameters on $\omega, \nu, \mu_{\text{root}}, \zeta_{\text{root}}, \sigma_\mu^2$ and σ_ζ^2, allow us to explore our model's parameter space using Gibbs sampling. We used multiplier proposals for evolutionary rates and uniform sliding windows ω, ν and variance and mean at the root.

Model validation

We used simulations to test the ability of our model to differentiate between evolutionary processes and to determine whether the estimation of our model's parameters was accurate. We simulated the random evolution of a trait's mean and log standard deviation along a set of random phylogenetic trees and simulated asymmetric inheritance at every node with random switch parameters ($\boldsymbol{S_\omega}, \boldsymbol{S_\nu}$). We simulated five alternative scenarios that represented different evolutionary processes at speciation: (1) Symmetric and conserved inheritance ($\nu = 0, \omega = 0$, Fig. 1.a); (2) Symmetric and displaced inheritance ($\nu = 0, \omega = 0.5$, Fig. 1.c); (3) Asymmetric and conserved inheritance ($\nu = 0.5, \omega = 0$, Fig. 1.b); (4) Asymmetric and displaced inheritance ($\nu = 0.5, \omega = 0.5$, Fig. 1.d); (5) Intermediate asymmetric and displaced inheritance ($\nu = 0.2, \omega = 0.2$)).

We simulated each scenario on a set of phylogenetic trees containing a different number of species ($n = \{20, 50, 100\}$) and different evolutionary rates ($\sigma^2_\mu = \sigma^2_\zeta = \{0.1, 0.5, 1\}$). We generated trees using the *phytools* package based on a pure birth process with a root age fixed at 1 (Revell, 2012). We simulated phenotypic distributions using the bite package (Gaboriau et al., 2020) with the addition of ancestral distribution's inheritance process as described above. In total, each set of $(\omega, \nu, n, \sigma^2_\mu, \sigma^2_\zeta)$ was simulated 100 times leading to 4,500 simulations.

We analyzed simulated datasets by running 500,000 MCMC iterations, sampling every 100 iterations, and using uniform priors $\mathcal{U}(0, 0.99)$ for ω and ν, gamma priors $\Gamma(shape = 1.1, scale = 0.1)$ for evolutionary rates and normal priors for root values ($\theta_\mu : \mathcal{N}(\bar{\mu}, 2 * sd(\mu)), \theta_\mu : \mathcal{N}(\bar{\zeta}, 2 * n * sd(\zeta))$, see subsection Parameter estimation for an explication of the procedure to estimate parameters). We verified the convergence of the chains using Tracer v1.7.1 (Rambaut et al., 2018) and estimated the means and 95% credible interval of our parameters after removing the first 50,000 iterations as a burn-in. To test whether ω and ν significantly exceed 0 (under the null hypothesis of a fully symmetric and conserved inheritance), we implemented a Bayesian variable selection

algorithm where ν and ω are multiplied indicators ($I_\nu, I_\omega \in \{0, 1\}$) (see Silvestro et al. (2019) and Pimiento et al. (2020) for a similar implementation). The role of the indicators is thus to remove the effect of ω or ν when their value is 0 (in which case the model reduces to a standard Brownian motion), leaving them unaltered when they are set to a value of 1. The value of the indicators is assumed to be unknown and sampled along with the other parameters via MCMC. We set the prior probability to $P(I = 1) = 0.05$, meaning that we place a 0.95 probability on a regime with symmetric and conserved inheritance. Based on the posterior sampling frequencies of the indicators, we can estimate Bayes factors to assess the support for models with $\omega > 0$ or $\nu > 0$ using posterior odds divided by prior odds (Kass and Raftery, 1995), e.g., for the parameter ω:

$$BF = \frac{P(I_\omega = 1|\theta)}{1 - P(I_\omega = 1|\theta)} / \frac{P(I_\omega = 1)}{1 - P(I_\omega = 1)} \tag{0.12}$$

A $2\log(BF) > 6$ supports the relevance of ω and ν being different from 0 against a symmetric and conserved inheritance ($\omega = \nu = 0$) at speciation.

We also performed a series of control simulations to assess the presence of potential biases. We simulated the effect of an Ornstein-Uhlenbeck model (Hansen, 1997) on ζ to test the ability of our model to reject asymmetric and displaced inheritance in a dataset generated by an Ornstein-Uhlenbeck process.

In the absence of extinct lineages, our model can only capture asymmetric and displaced inheritance at nodes that are sampled in the phylogenetic tree. Non-sampled nodes due to extinction could create biases in our estimations. Similarly, incomplete sampling of extant species also leads to an incomplete representation of the internal nodes in a tree. To assess the effects of these factors on the estimation of the parameters of our model, we generated additional datasets with various extinction rates ($\mu = \{0.2, 0.5, 0.8\}$) and different levels of taxon sampling ($p = \{50\%, 66\%, 80\%\}$) under the five alternative inheritance scenarios described above.

Finally, we simulated the effect of process heterogeneity along the tree. We mapped regimes along the trees by randomly assigning alternative inheritance scenarios to the

tree's nodes. We generated datasets with different proportions of nodes under the null model (*i.e* $\nu = 0, \omega = 0; p = \{0.2, 0.5, 0.8\}$. Other nodes were simulated under the four other alternative scenarios. For all these control simulations, we fixed the number of tips to $n = 20$ and evolutionary rates to $\sigma^2_\mu = \sigma^2_\zeta = 0.1$. We ran MCMC chains and estimated Bayes Factors and parameters as described above.

Application Darwin's finches

Ecologists and evolutionary biologists often use Darwin's finches and other Coerebinae to illustrate adaptive radiation driven by character displacement (Grant and Grant, 2008). From a single granivore ancestor, the Coerebinae rapidly diversified in the Galapagos into a diverse clade and covered as many diets as the rest of the Thraupidae family (Reaney et al., 2020) thanks to their considerable diversity of beak shapes. Previous works often link the ecological opportunity brought by the colonization of oceanic islands with this rapid diversification (Grant and Grant, 2008; Reaney et al., 2020; Tobias et al., 2020). However, it remains unclear whether the speciation process is associated with accelerated evolutionary rates of beak shape caused by competition or whether it remained constant during Coerebinae diversification (Tobias et al., 2020). We use the ABM model to test for accelerated evolutionary rates at speciation in Coerebinae. We obtained data for the beak morphology of Coerebinae's individuals from each extant species (total culmen, beak nares, beak depth and beak width, Fig. 2) (Pigot et al., 2020) and a time-calibrated phylogenetic tree of the clade ($n = 14$; Burns et al., 2014). We ran two independent MCMC chains for 1,000,000 iterations, sampling every 100 iterations for each trait and discarding 100,000 iterations as a burn-in. To determine whether our data shows a signal of asymmetric or displaced inheritance, we employed the variable selection approach for ν and ω and estimated Bayes factors. We ran two independent chains with fixed indicators for parameter estimation according to the model selection procedure described above. We then calculated mean posterior estimates of our parameters.

Fig. 2. Beak morphology distributions per species in Coerebinae. The left represents the time-calibrated phylogeny of Coerebinae and the right panels represent estimated trait distributions from individual observation (dots) for each species and each trait used in the analysis

Results

Performance of the ABM model

Our simulations showed that the signal from different modes of cladogenetic trait inheritance, including trait asymmetry and displacement, can be correctly identified with the ABM model using Bayes factors tests under a range of scenarios. Our analyses resulted in the accurate identification of asymmetric and/or displaced scenarios ($BF_\nu > 6$ for simulations with $\nu > 0$, $BF_\omega > 6$ for simulations with $\omega > 0$) at low evolutionary rates ($\sigma^2_\mu \leqslant 0.5$; Fig. 3). Likewise, asymmetry and displacement were correctly rejected in simulations with $\nu = 0$ and/or $\omega = 0$ and low evolutionary rates.

However, the model was less reliable in consistently rejecting asymmetry in simulations with $\nu = 0$ and high evolutionary rates ($\sigma^2_\mu = 1$). Asymmetry was supported in 31% of simulations with $\nu = 0$ and $\sigma^2 = 1$. Support for displacement was lower in simulations that also included asymmetry (*i.e.* $\omega > 0$ and $\nu > 0$) and high evolutionary rates. Support for asymmetry and displacement increased in the case of stabilizing selection for intraspecific variance (OU model), an evolutionary mode currently not implemented in the ABM framework. The number of tips had a negligible effect on model identification.

We found that among simulations with high evolutionary rates, 40% of the chains failed to reach convergence with strong fluctuations in the posterior samples of the evolutionary rates (Fig. A14). These runs often led to an overestimation of the evolutionary rates and the erroneous rejection of asymmetric or displaced inheritance. We interpret these results as the result of non-identifiability of the ABM model parameters at extreme evolutionary rates. Model testing through Bayes factors therefore correctly identified instances of cladogenetic asymmetries and displacement (or their absence) in

cases of relatively low evolutionary rate. In contrast, extreme evolutionary rates appeared to weaken the signal.

Fig. 3. Variable selection results on the simulated datasets. The upper panel represents the $2log(BF)$ of asymmetric vs symmetric inheritance in function of the simulated scenarios. The lower panel represents the $2log(BF)$ of displaced vs conserved inheritance in function of the simulated scenarios. Most simulations involving displacement led to a $log(BF_\omega) > 6$. Most simulations involving asymmetry led to a $log(BF_\omega) > 6$. Simulations with high evolutionary rates led to less accurate model selection. Asym/Cons : Asymmetric and Conserved Inheritance ($\nu = 0.5, \omega = 0$); Asym/Dis(+) : Asymmetric and Displaced inheritance ($\nu = 0.5, \omega = 0.5$); Asym/Dis(-) : Intermediate scenario ($\nu = 0.2, \omega = 0.2$); OU : Sym/Cons with Ornstein-Ulhenbeck on the ζ ($\nu = 0, \omega = 0$); Sym/Cons : Symmetric and Conserved Inheritance ($\nu = 0, \omega = 0$); Sym/Dis : Symmetric and Displaced Inheritance ($\nu = 0, \omega = 0.5$).

The accuracy of parameter estimation varied depending on the simulation scenarios, but in most cases, the estimation of ω, ν and root state were accurate and unbiased (Fig. 4,A15). The accuracy of parameter estimation decreased with increasing evolutionary rates leading to either over or under-estimation depending on the parameter. In particular, we observed that ω tended to be underestimated for high levels of displacement, asymmetry, and evolutionary rates. We also observed stronger correlation among the posterior samples of the parameters with this scenario (Fig. A17, A19, A18, **??**), which indicates the difficulty to differentiate whether a fast change in phenotypic distribution is due to anagenetic or cladogenetic changes. Additionally, in the case of stabilizing selection for the intraspecific variance (OU), we observed an overestimation of ν and σ^2_μ. Here again, the number of tips did not affect parameter estimation. The Gibbs sampling procedure accurately estimates ancestral states and switch parameters at the tree's internal nodes, despite increased uncertainties for simulations with high evolutionary rates (Fig. A16).

The Bayes factor procedure and the parameter estimation remained robust to low levels of extinction (Fig. 5), incomplete taxon sampling (Fig. A27) and heterogeneity of the inheritance process (Fig. **??**). With higher extinction rates ($\lambda = 1$, $\mu = 0.5$ and $\mu = 0.8$), support for displacement decreased with respectively 74% and 36% of simulations with displacement showing a $BF > 6$ for $\omega > 0$. This decrease was associated with an overestimation of ν and σ^2_ζ (Fig. 5.d,f), and an underestimation of ω (Fig. 5.e). Conversely, support for asymmetry decreased in simulations with a high probability of symmetric and

conserved inheritance at dichotomies ($p = 0.8$, 39%, Fig. **??**) and increased in simulations with symmetry and high incomplete taxon sampling. Up to 48% simulations ran with 50% of missing taxa and symmetric and displaced inheritance ($\nu = 0$ and $\omega > 0$) show support for asymmetry (Fig. A27).

Fig. 4. Parameter estimation on the simulated datasets. Each panel represents mean parameter estimation in function of the simulated scenario. The grey dashed lines represent the parameter value used to simulate the dataset. Asym/Cons : Asymmetric and Conserved Inheritance ($\nu = 0.5, \omega = 0$); Asym/Dis(+) : Asymmetric and Displaced inheritance ($\nu = 0.5, \omega = 0.5$); Asym/Dis(-) : Intermediate scenario ($\nu = 0.2, \omega = 0.2$); OU : Sym/Cons with Ornstein-Ulhenbeck on the ζ ($\nu = 0, \omega = 0$); Sym/Cons : Symmetric and Conserved Inheritance ($\nu = 0, \omega = 0$); Sym/Dis : Symmetric and Displaced Inheritance ($\nu = 0, \omega = 0.5$).

Coerebinae evolution

We found strong support ($log(BF_\omega) > 6$) for cladogenetic displacement in three out of four beak traits (Tab. 1). Specifically, we found evidence for displaced inheritance of total culmen, bill nares, and bill depth, although the estimated values of ω for the first two were low. In contrast, we found a consistent rejection of asymmetric inheritance for all traits with negative log BF values indicating strong support for $\nu = 0$ (Tab. 1). We also observe values of similar magnitude across all traits for the estimates of μ_{root}, σ^2_μ and σ^2_ζ, while the estimated ζ_{root} are much lower for bill width than for any other traits relative to observed ζ in present species. We checked that our model was not biased by an OU evolutionary regime on ζ, using the JIVE model from the R-package *bite* (Gaboriau et al., 2020). We tested for alternative evolutionary regimes on ζ and concluded that our dataset showed no support for an OU on ζ (Tab. S1).

Discussion

Evolutionary processes are all constrained by the ability of individuals to transmit their genes to the next generation. Most forces affecting evolution (e.g., selection) therefore unfold their effects at the individual level (Lande, 1976; Hallgrímsson and Hall, 2005;

Kaliontzopoulou et al., 2018). Nevertheless, current phylogenetic comparative methods attempting to estimate these forces at a macro-evolutionary scale make the simplifying assumption that species, not individuals, are the fundamental unit of evolutionary mechanisms driving trait evolution. This assumption is grounded on reducing mathematical complexity rather than on theoretical expectations and can lead to biased estimates (Duchen et al., 2021). Using species as the unit of phenotypic variation reduces our ability to model drift, mutation and recombination, which are thought to be the main forces generating variation at the microevolutionary scale (Mayr, 1963; Lande, 1976) and recent methodological developments showed that incorporating intraspecific trait variance in the model can substantially improve our understanding of traits within and among species (Kostikova et al., 2016; Gaboriau et al., 2020). However, even these models assume that speciation is an instantaneous event and that the full distribution of ancestral phenotypes is inherited by the descendants without modifications. This assumption limits the possibility of testing for the effect of divergence on trait evolution (Schluter, 2000; Turelli et al., 2001; Bokma, 2008; Duchen et al., 2021), as proposed by the punctuated-equilibrium theory more than 50 years ago (Eldredge and Gould , 1972).

In this study, we presented a model that relaxed some of these assumptions, providing a framework to infer how a trait (and its intraspecific variation) may be asymmetrically inherited by descendent species, reflecting different magnitudes of trait displacement at speciation. Even though our model is not individual-based, it incorporates multiple measurements per species and allows us to model the evolution of a trait mean and variance, thus approximating intraspecific variation. Our framework thus integrates elements of micro-evolutionary models scaled up to macroevolutionary scales. Our ABM captures the signal of trait segregation at speciation, which can be interpreted as the result of different mechanisms, such as trait-based segregation, random segregation, or segregation caused by environmental gradients. For instance, one can expect the negative switch parameters (*i.e.* a parameter value indicating the lineage inherits a smaller

proportion of ancestral variation) to be associated with specialization events or peripatric speciation.

Unlike previous models allowing for random jumps in phenotypes (Bokma , 2002; Bokma, 2008; Landis et al., 2013; Landis and Schraiber , 2017(@), the ABM model incorporates jumps within a constrained range, determined by an estimated intra-specific phenotypic variance. Thus, the ancestral distribution inheritance process allows the modeling of fast character displacement realistically in the light of the modern synthesis instead of considering stochastic cladogenetic jumps. Indeed, the ABM approximates the effect of several micro-evolutionary processes associated with the speciation process. For instance, character displacement with low overlap between descendants distribution can be the effect of disruptive selection associated with assortative mating (Dieckman et al., 2004; Seehausen and Van Alphen, 1999; Bolnick, 2001; Gavrilets, 2003; Dijkstra and Border, 2018; Tobias et al., 2014). Alternatively, the isolation of small populations following a colonisation event can lead to an asymmetric inheritance of the ancestral variance. In turn, local adaptation can cause rapid evolution of remote populations leading to significant displacement (Simpson, 1953; Losos and Ricklefs, 2009; Wagner et al., 2012; Mahler et al., 2013). In this context, the ancestral variance does not represent the realised variance of ancestral populations but more the evolvability of ancestral species (Wagner and Altenberg, 1996; Abzhanov, 2017; Payne and Wagner, 2019), meant here as the genetic potential to create diversity as a response to selection drift and recombination. Because evolvability depends on genetic and structural constraints (Pigliucci, 2008), it can be seen as a heritable trait and modeled as a diffusion process (Kostikova et al., 2016; Gaboriau et al., 2020). Furthermore, speciation events associated with character displacement and specialisation can reduce the evolvability of descendant species and lead to the realised phenotypic variance that we observe today.

Model performance

Our simulations suggest that the ABM model can identify homogeneous regimes of cladogenetic asymmetric inheritance of the variance and displaced inheritance of the mean. Our variable selection algorithm allows rejecting the hypothesis of asymmetry (ν) or displacement (ω) when their signal is absent or weak. However, high anagenetic evolutionary rates can mask the signal of asymmetric or displaced inheritance, leading to model misidentifications. The rejection of displacement is conservative, meaning that the ABM model does not typically find spurious evidence. In contrast, the signal of asymmetric inheritance bears the same signal as high evolutionary rates. However, rates of anagenetic evolution that mask the signal of symmetric and displaced inheritance are high and generate the same signal as white noise, erasing the covariance between species. When the mean or the variance of a trait can evolve more than the amount of ancestral variance during the time separating the speciation event and present, any signal of asymmetry becomes erased. Estimating the proportion of nodes that satisfy this condition can give good indications on whether a dataset lies in that particular case. the phylogenetic We also show that the effect of stabilising selection on the log variance, modeled here as an OU process, also decreases the power of our model while increasing the uncertainty ranges in the estimated parameters. The ABM model is also robust to extinction, incomplete taxon sampling, and heterogeneity of the cladogenetic process. Model misidentification only increases for high values of extinction rates, low taxon sampling, and high heterogeneity. In contrast to the OU process, these sources of misidentification give support to the null model (symmetric and conserved inheritance) and reduce the ABM to a standard trait evolution model.

We also found that the number of tips considered has a low effect on the parameter estimation or variable selection procedure. We base this observation on simulations of a constant ν and ω across all nodes. With empirical datasets, the chances that this

Fig. 5. Variable selection results on datasets simulated with extinction. The upper panel (a.) represents the $2log(BF)$ of asymmetric vs symmetric inheritance in function of the simulated scenarios. The lower panel represents the $2log(BF)$ of displaced vs conserved inheritance in function of the simulated scenarios. Asym/Cons : Asymmetric and Conserved Inheritance ($\nu = 0.5, \omega = 0$); Asym/Dis(+) : Asymmetric and Displaced inheritance ($\nu = 0.5, \omega = 0.5$); Asym/Dis(-) : Intermediate scenario ($\nu = 0.2, \omega = 0.2$); Sym/Dis : Symmetric and Displaced Inheritance ($\nu = 0, \omega = 0.5$). Right Panels (c-e): Parameter estimation on the simulated datasets with extinction for the Asymmetric and Displaced Inheritance scenario (($\nu = 0.5, \omega = 0.5$). Each panel represents mean parameter estimation. The grey dashed lines represent the parameter value used to simulate the dataset.

hypothesis is violated increase with the number of tips, as heterogeneous evolutionary regimes are more likely in larger datasets. However, it is essential to note that standard phylogenetic comparative methods also make the hypothesis that trait inheritance at speciation is homogeneous across all nodes and that it is symmetric and conserved. As such, the ABM improves the standard BM process and opens promising perspectives in integrating individual-level processes in macro-evolutionary analyses.

Phenotypic evolution in Darwin's finches

The ABM model identified consistent character displacement and variance partitioning in traits associated with beak shape in Darwin's finches. This finding indicates that speciation in this well-known group of birds is associated with cladogenetic divergence of beak shape, likely linked to niche partitioning (Felice et al., 2019). It also demonstrates that the intra- and interspecific variation in Darwin's finches' beak shape is not only driven by anagenetic changes but is also the result of local adaptation happening simultaneously with allopatric speciation (Tobias et al., 2020) or divergence driven by competition or other interactions (Quintero et al. , 2020). This pattern is consistent with previous studies finding an association between elevated speciation rates and fast morphological evolution in Darwin's finches (Reaney et al., 2020). It further provides indirect evidence of the link between speciation and niche partitioning at the macroevolutionary scale for this clade.

Although the estimated values for ω are comparatively small, the displacement of descendants' mean phenotypes during speciation represents a $\approx 10\%$ of the ancestral 95% interval (or more if we consider the frequent underestimation of ω detected in our

simulations). It is thus likely that true displacement and variance partitioning are higher than estimated. We also observed that estimated variances at the root are substantially higher for the three traits under a regime of $\omega > 0$. This difference comes from the assumption of the ABM model that the regimes are constant through all nodes. A model with $\omega > 0$ or $\nu > 0$ thus assumes that the intraspecific variance divides at each node. The high morphological variation in Darwin's finches has often been associated with their high cranial shape modularity (Tokita et al., 2017; Abzhanov, 2017) and the high variability in their development (Mallarino et al., 2012). The high ancestral variance estimated can thus be associated with that evolutionary potential (*i.e.* evolvability) progressively constrained by competitive interactions every time a new species arises.

Future improvements to the ABM model

With the current implementation, the ABM only considers constant and neutral anagenetic evolution. The ABM model also assumes currently homogeneous regimes of cladogenetic trait inheritance. This assumption is unlikely to hold in nature as many factors are involved in the speciation processes that can generate heterogeneous patterns of trait distribution inheritance at the time of speciation. Therefore it can only identify broad tendencies without being precise about that heterogeneity. These limitations explain the progressive reduction of intraspecific variances predicted by the ABM in speciose clades when $\omega > 0$ (Fig. A3, Tab.1). This intraspecific variance reduction can be compared to the prediction of a niche space filling model associated with specialisation (Simpson, 1953; Pontarp , 2021) but quickly becomes unrealistic when including numerous nodes. Allowing other existing modes of anagenetic evolution (time-variation, selective optima, density dependence, evolutionary trend) would increase the flexibility of the model and could tackle some issues, such as the effect of stabilising selection on the log variance and the underestimation of ω. One straightforward solution could also be to allow for several regimes of cladogenetic trait distribution inheritance in the same way as existing

comparative methods. Those regimes could be introduced *a priori* using alternative knowledge about the clades evolution (Beaulieu et al., 2012; Zhang et al., 2022) or found based on the data (Uyeda and Harmon, 2014). Alternatively, we could extend this model to allow for the dependency between ν and ω on predictor variables. For instance, the effect of present geographical overlap could be used as a predictor of character displacement, while species densities could predict asymmetry.

Finally, the model assumes that every speciation event is observed in the phylogeny, ignoring the effect of extinction. Incorporating speciation and extinction rates and the effect of hidden speciation events would likely improve the predictions of the ABM model (Bokma, 2008) , even though our simulations showed that the model is robust to a moderate level of extinction. Furthermore, the asymmetric inheritance process represents a discrete realisation of a continuous event: speciation. The asymmetric and displaced inheritance described by the model is thus an abstraction of a continuous process of divergence from the ancestral distribution into two independent descendant distributions. This abstraction has some limitations, as it assumes that every speciation event happens at the same pace. Indeed, this assumption can be problematic as we expect a causal link between descendant distribution divergence and time to complete speciation. Introducing the concept of protracted speciation (Rosindell et al., 2010; Hua et al., 2022) in the ABM framework would allow taking into account the gradual nature of the speciation process and model a gradual divergence of daughter species distributions. However, the identification of this process might be difficult.

Overall, the ABM brings comparative methods one step closer to integrating individual variation into macro-evolutionary models. This is timely because phenotypic and phylogenetic datasets are growing in size and completeness, making it increasingly easy to obtain information about individual variation in traits for entire clades (see Tobias (2022); Schleuning et al. (2023)). The unprecedented accessibility of individual-level data across large numbers of species gives us the opportunity to incorporate individual variation

519 at the macro-evolutionary scale. It highlights the need for a new generation of models
520 designed to test individual-level predictions. By addressing one aspect of this challenge, we
521 hope that the ABM can inspire further progress in developing the models required to
522 explore emerging patterns in macroevolutionary diversification.

Acknowledgments

We declare that we have no conflict of interest to disclose.

D.S. received funding from the Swiss National Science Foundation (PCEFP3_187012), the Swedish Research Council (VR: 2019-04739), and the Swedish Foundation for Strategic Environmental Research MISTRA within the framework of the research programme BIOPATH (F 2022/1448). N.S. received funding from the Swiss National Science Foundation (310030_185223) and the University of Lausanne. We thank the DCSR of UNIL for the computing infrastructure used for this work.

Data Availability

Data available from the Dryad Digital Repository: https://doi.org/10.5061/dryad.q573n5tns. The latest version of the ABM model is in the GitHub repository: theogab/ABM

References

Abzhanov, A. 2017. The old and new faces of morphology: The legacy of D'Arcy Thompson's 'theory of transformations' and 'laws of growth'. Development (Cambridge) 144:4284–4297.

Ackermann, M. and M. Doebeli. 2004. Evolution of Niche Width and Adaptive Diversification. Evolution 58:2599–2612.

Beaulieu, J. M., D.-C. Jhwueng, C. Boettiger, and B. C. O'Meara. 2012. Modeling Stabilizing Selection: Expanding the Ornstein-Uhlenbeck Model of Adaptive Evolution. Evolution 66:2369–2383.

Blomberg, S. P., T. Garland, and A. R. Ives. 2003. Signal in Comparative Data : Testing for Phylogenetic Behavioral Traits Are More Labile. Evolution 57:717–745.

Eldredge, N. and S. J. Gould. 1972. Punctuated Equilibria: An Alternative to Phyletic Gradualism. Pages 82–115 in Models in Paleobiology (T. Schopf and J. Thomas, eds.) freeman, c ed. San Francisco.

Bokma, F. 2002. Detection of punctuated equilibrium from molecular phylogenies. Journal of Evolutionary Biology 15:1048–1056.

Landis, M. J. and J. G. Schraiber. 2017. Pulsed evolution shaped modern vertebrate body sizes. Proceedings of the National Academy of Sciences 0:201710920.

Quintero, I., M. J. Landis, and M. Hahn. 2020. Interdependent Phenotypic and Biogeographic Evolution Driven by Biotic Interactions. Systematic Biology 69:739–755.

Bokma, F. 2008. Detection of "punctuated equilibrium" by Bayesian estimation of speciation and extinction rates, ancestral character states, and rates of anagenetic and cladogenetic evolution on a molecular phylogeny. Evolution 62:2718–2726.

Bolnick, D. I. 2001. Intraspecific competition favours niche width expansion in Drosophila melanogaster. Nature 4:463–466.

Burns, K. J., A. J. Shultz, P. O. Title, N. A. Mason, F. K. Barker, J. Klicka, S. M. Lanyon, and I. J. Lovette. 2014. Phylogenetics and diversification of tanagers (Passeriformes: Thraupidae), the largest radiation of Neotropical songbirds. Molecular Phylogenetics and Evolution 75:41–77.

Castiglione, S., G. Tesone, M. Piccolo, M. Melchionna, A. Mondanaro, C. Serio, M. Di Febbraro, and P. Raia. 2018. A new method for testing evolutionary rate variation and shifts in phenotypic evolution. Methods in Ecology and Evolution 9:974–983.

Clavel, J. and H. Morlon. 2017. Accelerated body size evolution during cold climatic periods in the Cenozoic. Proceedings of the National Academy of Sciences 114:4183–4188.

Dieckman, U., M. Doebeli, J. A. J. Metz, and D. Tautz. 2004. Adaptive Speciation.

Dijkstra, P. D. and S. E. Border. 2018. How does male-male competition generate negative frequency-dependent selection and disruptive selection during speciation? Current Zoology 64:89–99.

Drury, J., J. Clavel, M. Manceau, and H. Morlon. 2016. Estimating the effect of competition on trait evolution using maximum likelihood inference. Systematic Biology 65:700–710.

Duchen, P., M. L. Alfaro, J. Rolland, N. Salamin, and D. Silvestro. 2021. On the Effect of Asymmetrical Trait Inheritance on Models of Trait Evolution. Systematic Biology 70:376–388.

Duchen, P., C. Leuenberger, S. M. Szilágyi, L. Harmon, J. Eastman, M. Schweizer, and D. Wegmann. 2017. Inference of Evolutionary Jumps in Large Phylogenies using Lévy Processes. Systematic Biology 66:950–963.

Eastman, J. M., D. Wegmann, C. Leuenberger, and L. J. Harmon. 2013. Simpsonian

584 'Evolution by Jumps' in an Adaptive Radiation of Anolis Lizards. ArXiv
585 Page 1305.4216.

586 Felice, R. N., J. A. Tobias, A. L. Pigot, and A. Goswami. 2019. Dietary niche and the
587 evolution of cranial morphology in birds. Proceedings of the Royal Society B: Biological
588 Sciences 286:20182677.

589 Felsenstein, J. 1973. Maximum likelihood estimation of evolutionary trees from continuous
590 characters. American Journal of Human Genetics 25:471–492.

591 Felsenstein, J. 1985. Phylogenies and the Comparative Method.

592 Gaboriau, T., F. K. Mendes, S. Joly, D. Silvestro, and N. Salamin. 2020. A multi-platform
593 package for the analysis of intra- and interspecific trait evolution. Methods in Ecology
594 and Evolution 11:1439–1447.

595 Gavrilets, S. 2003. Perspective: Models of speciation - What have we learned in 40 years?
596 Evolution 57:2197–2215.

597 Gavrilets, S. 2014. Models of speciation: Where are we now? Journal of Heredity
598 105:743–755.

599 Grant, P. R. and R. B. Grant. 2008. How and Why Species Multiply: The Radiation of
600 Darwin's Finches. Princeton ed. Princeton University Press.

601 Hallgrímsson, B. and B. K. Hall. 2005. Variation and variability: Central concepts in
602 biology. Pages 1–7 *in* Variation. Elsevier Inc.

603 Hansen, T. F. 1997. Stabilizing Selection and the Comparative Analysis of Adaptation.
604 Evolution 51:1341.

605 Hansen, T. F., G. H. Bolstad, and M. Tsuboi. 2021. Analyzing Disparity and Rates of
606 Morphological Evolution with Model-Based Phylogenetic Comparative Methods.
607 Systematic Biology 0:1–19.

Harmon, L. J. and J. B. Losos. 2005. the Effect of Intraspecific Sample Size on Type I and Type Ii Error Rates in Comparative Studies. Evolution 59:2705–2710.

Harmon, L. J., J. B. Losos, T. Jonathan Davies, R. G. Gillespie, J. L. Gittleman, W. Bryan Jennings, K. H. Kozak, M. A. McPeek, F. Moreno-Roark, T. J. Near, A. Purvis, R. E. Ricklefs, D. Schluter, J. A. Schulte, O. Seehausen, B. L. Sidlauskas, O. Torres-Carvajal, J. T. Weir, and A. T. Mooers. 2010a. Early bursts of body size and shape evolution are rare in comparative data. Evolution 64:2385–2396.

Harmon, L. J., J. B. Losos, T. Jonathan Davies, R. G. Gillespie, J. L. Gittleman, W. Bryan Jennings, K. H. Kozak, M. A. McPeek, F. Moreno-Roark, T. J. Near, A. Purvis, R. E. Ricklefs, D. Schluter, J. A. Schulte II, O. Seehausen, B. L. Sidlauskas, O. Torres-Carvajal, J. T. Weir, and A. O. Mooers. 2010b. Early bursts of body size and shape evolution are rare in comparative data. Evolution 64:no–no.

Hua, X., T. Herdha, and C. Burden. 2022. Protracted speciation under the state-dependent speciation and extinction approach. Systematic Biology syac041.

Kaliontzopoulou, A., C. Pinho, and F. Martínez-Freiría. 2018. Where does diversity come from? Linking geographical patterns of morphological, genetic, and environmental variation in wall lizards. BMC Evolutionary Biology 18:124.

Kass, R. E. and A. E. Raftery. 1995. Bayes Factors and Model Uncertainty. Journal of American Statistical Association Pages 773–795.

Khabbazian, M., R. Kriebel, K. Rohe, and C. Ané. 2016. Fast and accurate detection of evolutionary shifts in Ornstein–Uhlenbeck models. Methods in Ecology and Evolution 7:811–824.

Kopp, M. 2010. Speciation and the neutral theory of biodiversity: Modes of speciation affect patterns of biodiversity in neutral communities. BioEssays 32:564–570.

Kostikova, A., D. Silvestro, P. B. Pearman, and N. Salamin. 2016. Bridging inter-and intraspecific trait evolution with a hierarchical Bayesian approach. Systematic Biology 65:417–431.

Lande, R. 1976. Natural Selection and Random Genetic Drift in Phenotypic Evolution. Evolution 30:314–334.

Lande, R. 1980a. Genetic Variation and Phenotypic Evolution During Allopatric Speciation. The American Naturalist 116:463–479.

Lande, R. 1980b. Microevolution in Relation to Macroevolution - Macroevolution: Pattern and Process. Steven M. Stanley W. H. Freeman and Co.; San Francisco. 1979. xi + 332 pp. $22.50. Paleobiology 6:233–238.

Landis, M. J., J. G. Schraiber, and M. Liang. 2013. Phylogenetic Analysis Using Lévy Processes: Finding Jumps in the Evolution of Continuous Traits. Systematic Biology 62:193–204.

Lartillot, N. and R. Poujol. 2011. A phylogenetic model for investigating correlated evolution of substitution rates and continuous phenotypic characters. Molecular Biology and Evolution 28:729–744.

Losos, J. B., M. Leal, R. E. Glor, K. De Queiroz, P. E. Hertz, L. Rodríguez Schettino, A. C. Lara, T. R. Jackman, and A. Larson. 2003. Niche lability in the evolution of a Caribbean lizard community. Nature 424:542–545.

Losos, J. B. and R. E. Ricklefs. 2009. Adaptation and diversification on islands. Nature 457:830–836.

Mahler, D. L., T. Ingram, L. J. Revell, and J. B. Losos. 2013. Exceptional convergence on the macroevolutionary landscape in island lizard radiations. Science 341:292–5.

Mallarino, R., O. Campàs, J. A. Fritz, K. J. Burns, O. G. Weeks, M. P. Brenner, and A. Abzhanov. 2012. Closely related bird species demonstrate flexibility between beak

morphology and underlying developmental programs. Proceedings of the National Academy of Sciences of the United States of America 109:16222–16227.

Mayr, E. 1963. Animal Species and Evolution. Harvard University Press, Harvard.

Mendes, F. K., J. A. Fuentes-González, J. G. Schraiber, and M. W. Hahn. 2018. A multispecies coalescent model for quantitative traits. eLife 7:1–24.

Pagel, M. 1999. Inferring the historical patterns of biological evolution. Nature 401:488.

Payne, J. L. and A. Wagner. 2019. The causes of evolvability and their evolution.

Pigliucci, M. 2008. Is evolvability evolvable?

Pigot, A. L., C. Sheard, E. T. Miller, T. P. Bregman, B. G. Freeman, U. Roll, N. Seddon, C. H. Trisos, B. C. Weeks, and J. A. Tobias. 2020. Macroevolutionary convergence connects morphological form to ecological function in birds. Nature Ecology and Evolution 4:230–239.

Pimiento, C., C. D. Bacon, D. Silvestro, A. Hendy, C. Jaramillo, A. Zizka, X. Meyer, and A. Antonelli. 2020. Selective extinction against redundant species buffers functional diversity: Redundancy buffers functional diversity. Proceedings of the Royal Society B: Biological Sciences 287.

Rambaut, A., A. J. Drummond, D. Xie, G. Baele, and M. A. Suchard. 2018. Posterior summarization in Bayesian phylogenetics using Tracer 1.7. Systematic Biology 67:901–904.

Reaney, A. M., Y. Bouchenak-Khelladi, J. A. Tobias, and A. Abzhanov. 2020. Ecological and morphological determinants of evolutionary diversification in Darwin's finches and their relatives. Ecology and Evolution 10:14020–14032.

Revell, L. J. 2012. phytools: An R package for phylogenetic comparative biology (and other things). Methods in Ecology and Evolution 3:217–223.

Rosindell, J., S. J. Cornell, S. P. Hubbell, and R. S. Etienne. 2010. Protracted speciation revitalizes the neutral theory of biodiversity. Ecology Letters 13:716–727.

Schleuning, M., D. García, and J. A. Tobias. 2023. Animal functional traits : Towards a trait- based ecology for whole ecosystems. Functional Ecology 37:4–12.

Schluter, D. 2000. The Ecology of Adaptive Radiation. Oxford ser ed. Oxford University Press.

Schwämmle, V., A. O. Sousa, and S. M. De Oliveira. 2006. Monte Carlo simulations of parapatric speciation. European Physical Journal B 51:563–570.

Seehausen, O. and J. J. Van Alphen. 1999. Can sympatric speciation by disruptive sexual selection explain rapid evolution of cichlid diversity in Lake Victoria? Ecology Letters 2:262–271.

Silvestro, D., N. Salamin, A. Antonelli, and X. Meyer. 2019. Improved estimation of macroevolutionary rates from fossil data using a Bayesian framework. Paleobiology 45:546–570.

Simpson, G. G. 1953. The Major Features of Evolution. Columbia u ed. University Presses of California, Columbia and Princeton, Columbia.

Tobias, J. A. 2022. A bird in the hand: Global-scale morphological trait datasets open new frontiers of ecology, evolution and ecosystem science. Ecology Letters 25:573–580.

Tobias, J. a., C. K. Cornwallis, E. P. Derryberry, S. Claramunt, R. T. Brumfield, and N. Seddon. 2014. Species coexistence and the dynamics of phenotypic evolution in adaptive radiation. Nature 506:359–363.

Tobias, J. A., J. Ottenburghs, and A. L. Pigot. 2020. Avian Diversity: Speciation, Macroevolution, and Ecological Function.

Tokita, M., W. Yano, H. F. James, and A. Abzhanov. 2017. Cranial shape evolution in adaptive radiations of birds: Comparative morphometrics of Darwin's finches and Hawaiian honeycreepers. Philosophical Transactions of the Royal Society B: Biological Sciences 372.

Pontarp, M. 2021. Ecological opportunity and adaptive radiations reveal eco-evolutionary perspectives on community structure in competitive communities. Scientific Reports 11:1

Turelli, M., N. H. Barton, and J. A. Coyne. 2001. Theory and speciation.

Uyeda, J. C. and L. J. Harmon. 2014. A Novel Bayesian Method for Inferring and Interpreting the Dynamics of Adaptive Landscapes from Phylogenetic Comparative Data. Systematic Biology 63:902–918.

Wagner, C. E., L. J. Harmon, and O. Seehausen. 2012. Ecological opportunity and sexual selection together predict adaptive radiation. Nature 487:366–369.

Wagner, G. P. and L. Altenberg. 1996. Perspective: Complex adaptations and the evolution of evolvability. Evolution 50:967–976.

Zhang, Q., R. H. Ree, N. Salamin, Y. Xing, and D. Silvestro. 2022. Fossil-Informed Models Reveal a Boreotropical Origin and Divergent Evolutionary Trajectories in the Walnut Family (Juglandaceae). Systematic Biology 71:242–258.

Variable	$2log(BF_\omega)$	$2log(BF_\nu)$	$\bar{\omega}$	$\bar{\nu}$	$\bar{\theta_\mu}$	$\bar{\theta_\zeta}$	$\bar{\sigma^2_\mu}$	$\bar{\sigma^2_\zeta}$
Total culmen	6.24	−4.35	0.09	-	14.53	13.60	0.96	0.37
Bill nares	6.14	−4.78	0.08	-	9.33	10.75	0.67	0.31
Bill width	1.10	−6.19	-	-	5.06	0.55	1.19	0.17
Bill depth	6.32	−5.25	0.91	-	6.36	14.93	1.18	0.42

Table 1. Results of the ABM model fitted on Darwin's finches beak shape traits. The log(BF) columns represent the results of MCMC chains ran with the variable selection algorithm. Estimated parameters (mean posterior) are calculated from MCMC chains ran with selected variables from the previous approach.

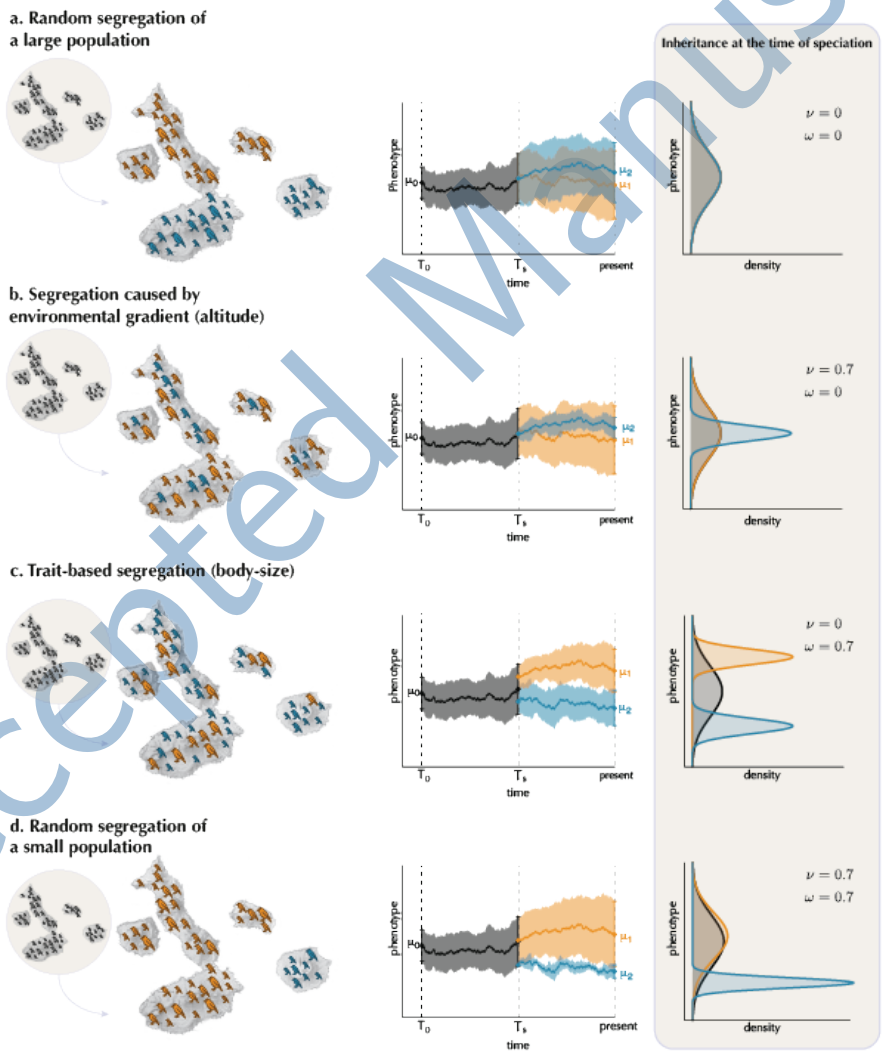

Fig. 1.

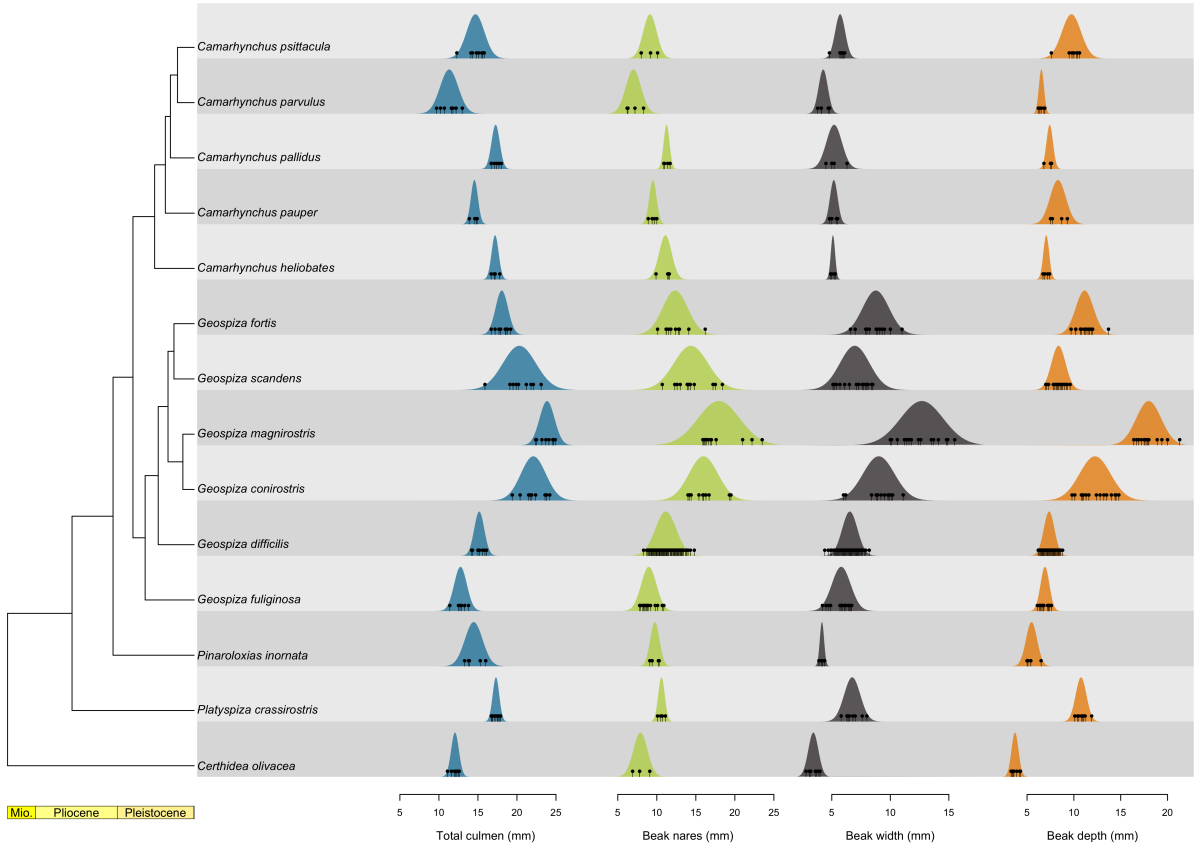

Fig. 2.

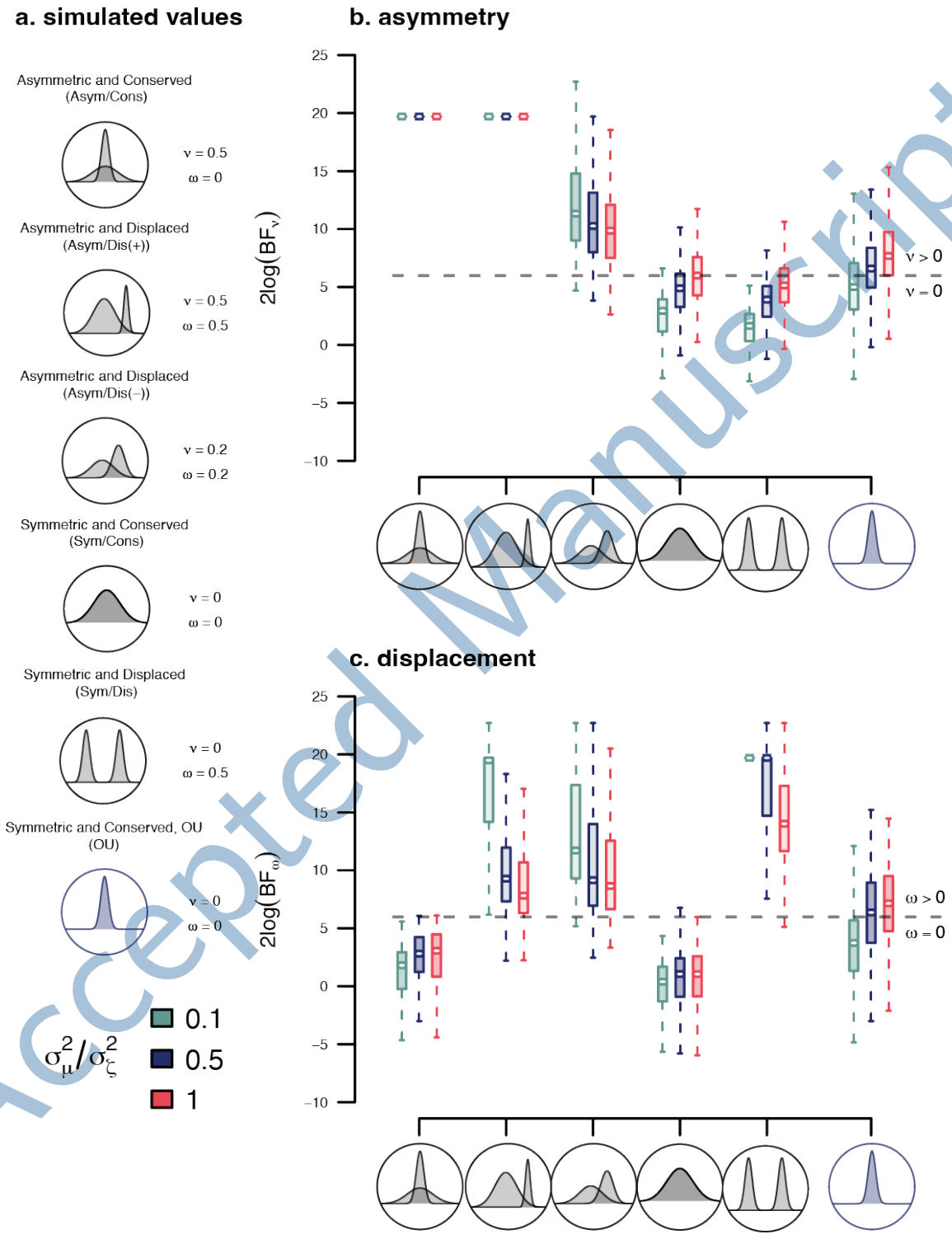

Fig. 3.

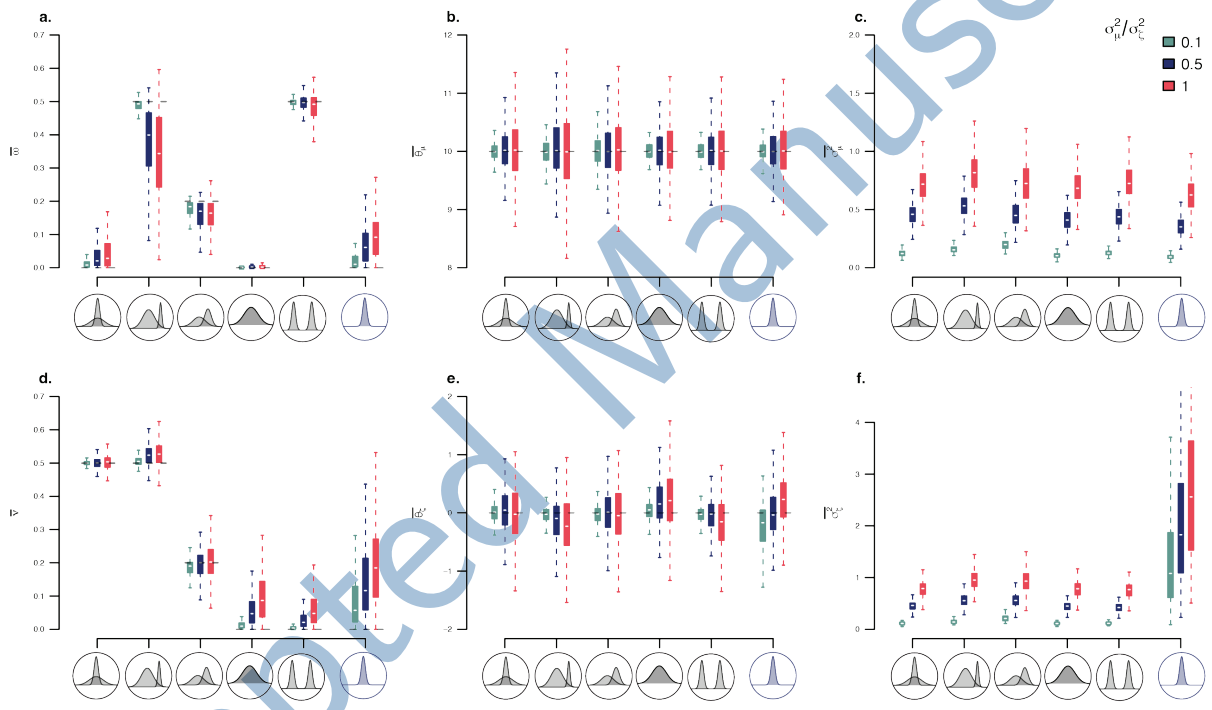

Fig. 4.

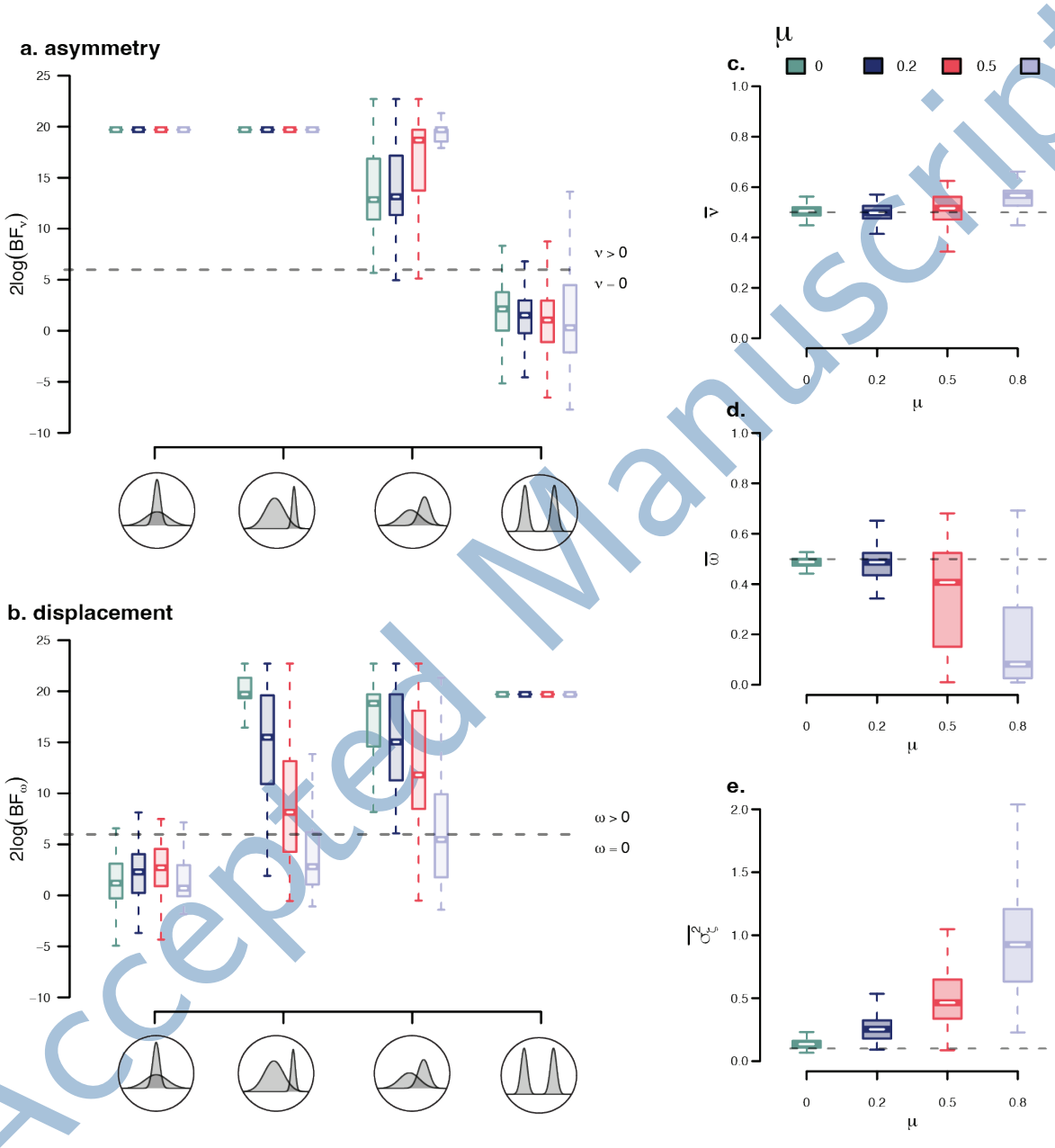

Fig. 5.